Simulation of a Hydraulic Actuator

Abstract: A simple mathematical model of a hydraulic actuator is formulated, and the differential equations describing the model are derived. Experimental data and a computational solution of the model are determined. Results correspond favorably with oscilloscope velocity traces; hence the model could serve a useful purpose in mechanical design.

Introduction

The purpose of the investigation described in this paper was to simulate the operation of one of the positioning systems used in the hydraulic actuator for the IBM 1301 Disk Storage Unit.¹ The actuator has two positioning systems: (1) the glob adder hydraulic system, which transfers a measured volume of fluid to the slave cylinder to move the slave piston, and (2) the piston adder, which moves the complete floating slave cylinder assembly shown in Fig. 1. The combined glob and piston adder motions give the load motion. In this paper we treat only the glob adder system.

The hydraulics for the actuator motion are contained in the closed system (Fig. 1) which connects the slave cylinder, shuttle valve, and glob adders. There are six glob adder pistons. One side of each piston is connected to a control valve. Each of the six control valves connects one of the pistons with either sump (20 psi) or system pressure (550 psi). Because the piston rod in the slave cylinder is biased by the system pressure acting on half the piston area, the pressure between the glob adders and the slave cylinder stabilizes at the end of every motion at half the system pressure. Therefore, changing a control valve from sump to system pressure will cause a displacement of the glob piston and hence the slave piston in the "out" direction, the length of the stroke depending on the volume displacement of the glob piston.²⁻⁵ Changing a control valve from system pressure to sump causes a similar displacement in the opposite "in" direction. The detent fixes the position of the slave piston rod after the glob adders have completed their strokes and corrects small positioning errors due to leakage.

A schematic model of the hydraulics is shown in Fig. 2. The orifice a(A) in the control valve connects the region

at the applied pressure P with Region A. Region A is in turn connected with B on the left by three parallel paths:

- (a) A check valve a(Bc) allows flow into the cylinder only.
- (b) A needle valve a(Bn) allows flow in both directions through a small adjustable orifice. The needle valve is used in the final tuning of the actuator.
- (c) An undercut a(Bu) also provides flow in both directions, as long as the glob piston does not cover it. The location of the undercut is such that the piston will cover it when the piston completes half of its stroke. Each glob piston has two damping cuts at each end. The purpose of these cuts is to provide a controlled deceleration of the glob piston and hence of the load.

Region C on the right of the glob piston is connected with Region D by three analogous paths, a(Cc), a(Cn), and a(Cu).

The following assumptions and approximations have been made to facilitate analysis:

- (a) Only the operation of the actuator before detenting is treated. Any motion of the shuttle valve before detenting is neglected. In this version of the model, leakage is also neglected.
- (b) The operating temperature can vary from the nominal 120°F; however, it is assumed that any one motion can be treated adiabatically.
- (c) An essentially one-dimensional lumped parameter model is treated. The equivalent orifice approximation is used. The theory is based on the continuity equation which assumes steady flow and thus certain dynamic

329

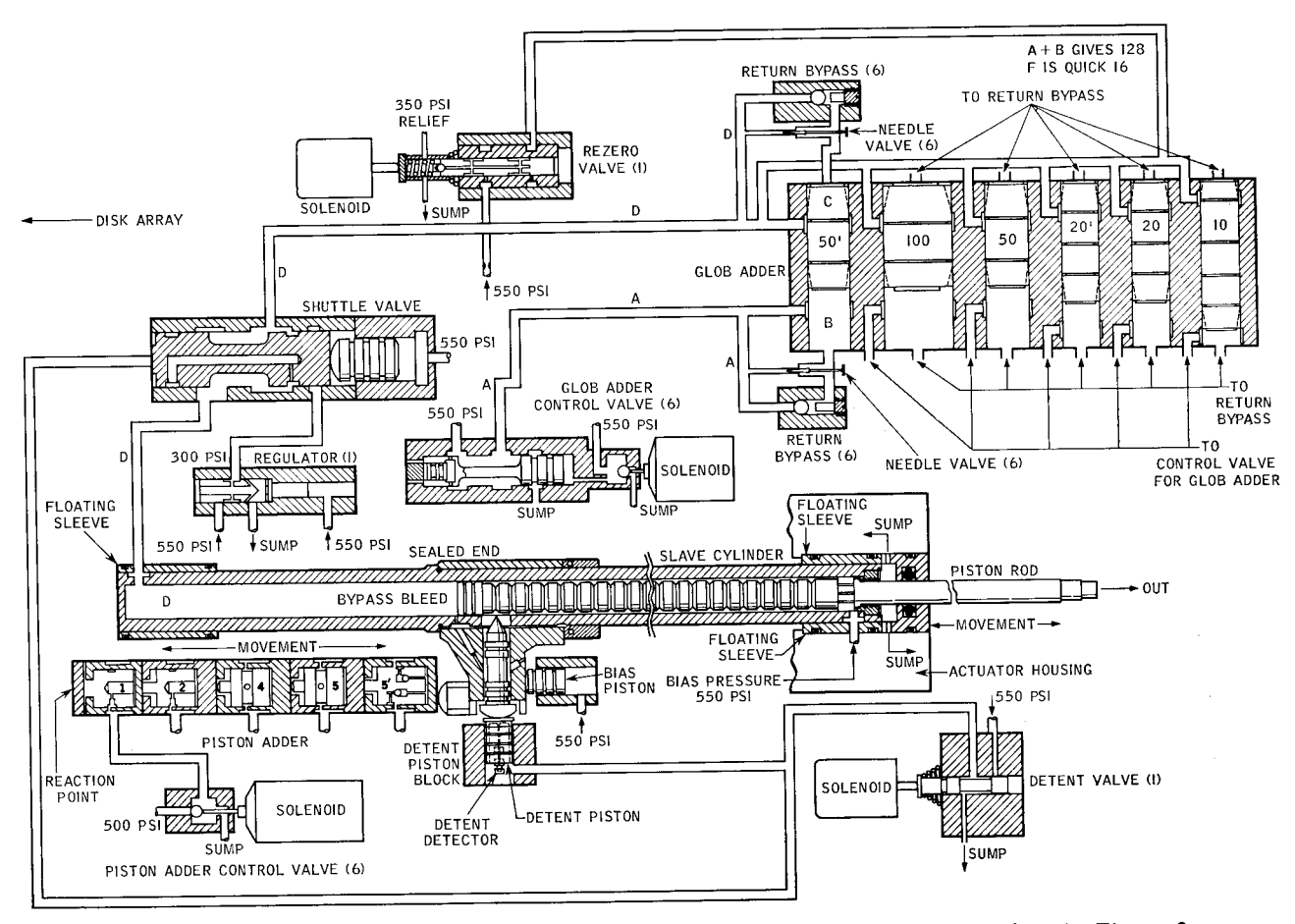
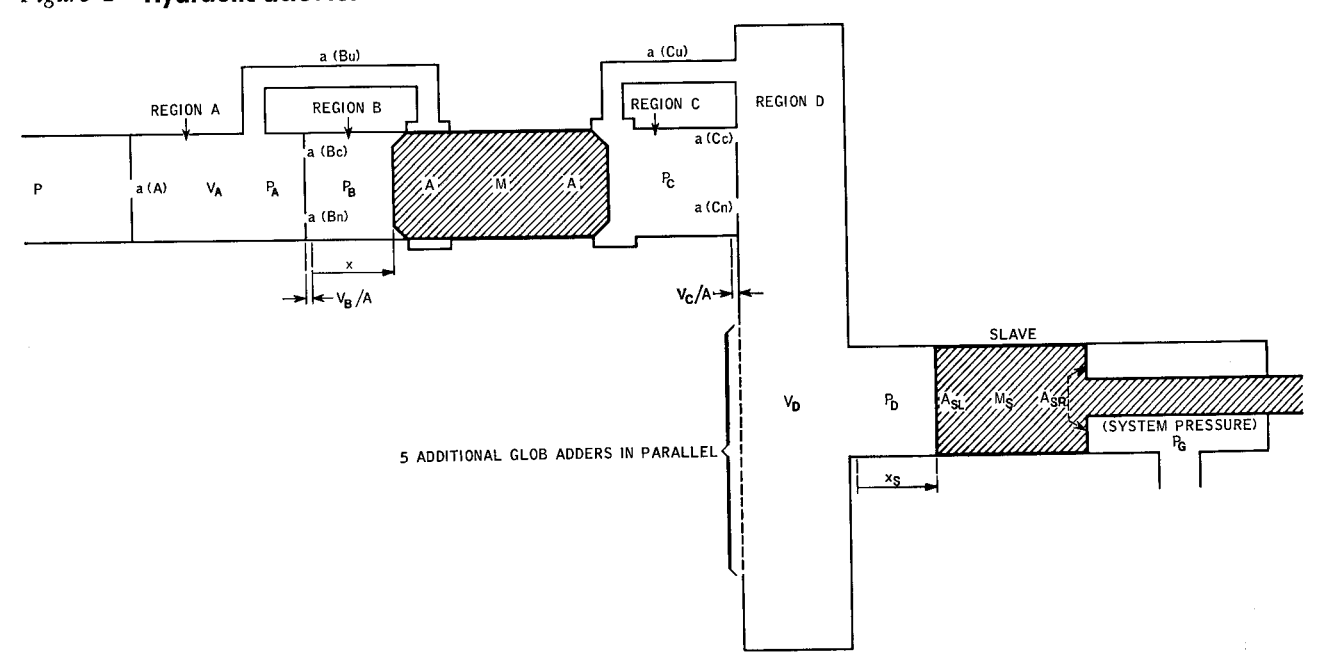


Figure 1 Hydraulic actuator schematic diagram. Regions A,B,C, and D are indicated as in Figure 2.





effects are neglected. However, pressure wave propagation need not be considered since the acoustic wave velocity is much greater than the maximum piston velocities. In treating the fluid, viscous and body forces are neglected. Also, the model does not have any provision for cavitation effects.

Analysis of the one-dimensional model

If we define⁶

$$f(P) = \int_{P_*}^{P} \frac{dP}{\rho(P)} \,, \tag{1}$$

where P is the pressure, ρ the weight density of the fluid, and P_* atmospheric pressure, then the fluid flow through an orifice (Fig. 3) between Regions A and B can be approximated by

$$G_{B} = \begin{cases} (ca)_{R} \rho(P_{B})[2g|f(P_{A}) - f(P_{B})]^{1/2} \\ \cdot \operatorname{sgn}(P_{A} - P_{B}) & \text{if} \quad P_{A} \geq P_{B} \\ (ca)_{L} \rho(P_{A})[2g|f(P_{A}) - f(P_{B})]^{1/2} \\ \cdot \operatorname{sgn}(P_{A} - P_{B}) & \text{if} \quad P_{A} < P_{B} \end{cases}$$
 (2)

Here c is the discharge coefficient of the orifice of area a, the subscripts R and L denote flow either to the right or to the left, and sgn (x) designates the sign of x:

$$sgn(x) = \begin{cases} +1 & \text{if } x > 0 \\ 0 & \text{if } x = 0 \\ -1 & \text{if } x < 0 \end{cases}$$
 (3)

The difference in f(P) has been used in (2) because the fluid is compressible, whereas for an incompressible fluid, (2) would involve a difference of P.

For a volume V at pressure P, the continuity equation states

Net flow
$$= \frac{d}{dt} \left[\rho(P) V \right]$$
$$= \dot{\rho} V + \dot{V} \rho. \tag{4}$$

The adiabatic bulk modulus of the fluid provides a relation between the density and the pressure derivatives:

$$R(P) = \rho \frac{dP}{d\rho} = \rho \frac{\dot{P}}{\dot{\rho}}.$$
 (5)

Substituting in (4),

$$\dot{P} = \frac{R(P)}{V} \left[\frac{\text{net flow}}{\rho(P)} - \dot{V} \right]. \tag{6}$$

Figure 2 reveals that the volume in Region A for every glob adder is constant, say V_A . Furthermore, the volumes

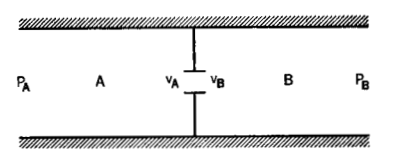


Figure 3 Orifice flow.

in Regions B and C are linearly dependent upon the position of the glob adder piston. If A is the area and L is the maximum glob piston displacement, and if x represents the displacement of the piston from rest (against the left end of the cylinder) $0 \le x \le L$, then the volume in Region B is $Ax + V_B$ and that in Region C is $A(L - x) + V_C$, where V_B and V_C represent small volumes remaining in Region B at Ax = 0 and in region C at Ax = 0, respectively. Now, if Ax = 0 and in region Ax = 0 and if Ax =

$$\dot{P}_A = \frac{R(P_A)}{V_A} \left[\frac{G_A - G_B}{\rho(P_A)} \right] \tag{7}$$

$$\dot{P}_B = \frac{R(P_B)}{Ax + V_B} \left[\frac{G_B}{\rho(P_B)} - A\dot{x} \right] \tag{8}$$

$$\dot{P}_C = \frac{R(P_B)}{A(L-x) + V_C} \left[\frac{-G_D}{\rho(P_C)} + A\dot{x} \right]$$
 (9)

The motion of a piston of mass M and area A with pressure P_B on the left and P_C on the right must, of course, obey Newton's second law:

$$\ddot{x} = \frac{1}{M} [(P_B - P_C)A - F \operatorname{sgn}(\dot{x})],$$
 (10)

where *F* is the frictional force acting on the mass.

Now we turn our attention to the slave piston. The volume in region D is linearly dependent upon the position of the slave piston. As before, application of (6) and Newton's second law yields

$$\dot{P}_D = \frac{R(P_D)}{A_{SL}x_S + V_D} \left[\sum_{\text{adders}} \frac{G_D}{\rho(P_D)} - A_{SL}\dot{x}_S \right] \quad (11)$$

$$\ddot{x}_S = \frac{1}{M_S} [P_D A_{SL} - P_G A_{SR} - F_S \operatorname{sgn} (\dot{x}_S)], \quad (12)$$

where A_{SL} and A_{SR} are the areas of the slave piston on the left and right, x_S is the position, M_S the mass, and F_S the frictional force.

Integration with respect to time of the system of Eqs. (7), (8), (9), (10), (11), and (12) yields curves for the variables x, P_A , P_B , P_C , x_S , and P_D , which completely describe our model. For any one motion there will be one

set of Eqs. (7), (8), (9), and (10) for every moving glob adder. For N moving glob adders, $1 \le N \le 6$, there are 4N + 2 equations to solve. Since the system is reduced to a first order one for numerical computation by the substitutions $y = \dot{x}$ and $y_S = \dot{x}_S$, the number of equations is actually 5N + 3. This number can be reduced by a consideration of the orifices in the model. In comparison to the others, the orifices in the check valves, a(Bc) and a(Cc), are large, as are the orifices of the undercuts, a(Bu) and a(Cu), when the glob adder piston does not partially cover them. The dynamic situation requires that the pressures in two regions separated by a large orifice tend to remain equal, so that we can to a good approximation combine the regions. Since a check valve allows flow into the cylinder only, it is clear that a(Bc)is closed for a glob instroke and similarly for a(Cc) on outstroke. Therefore, if every moving glob adder is classified as either an outstroke or an instroke, we can combine Region A into Region B, deleting (7) for the outstrokes, and combine Region C into Region D, deleting (9) for the instrokes. Thus, the number of equations is reduced to 4N + 3.

A further partial reduction in the number of equations to be integrated can be made if the motion of each glob adder is divided into two stages, acceleration and deceleration. The acceleration stage is approximately half of the motion, before the piston begins to block the undercut orifice. For an outstroke in acceleration the undercut a(Cu) is unblocked, and Region C can be combined into D, deleting (9). Similarly, for an instroke in acceleration (7) can be deleted. Of course, if a glob adder is stationary or has completed its stroke, its equations do not have to be considered. Thus, we have three equations for every glob adder in acceleration, four for every glob adder in deceleration, and three for the slave piston to be integrated at any time step.

Since P_G is constant (system pressure), P_D stabilizes at the end of every motion to $P_G(A_{SR}/A_{SL})$. This is then the initial condition for P_D and P_C . For an outstroke the applied pressure P is changed (linearly by assumption) from sump to system pressure in T seconds. Therefore, initial conditions for the glob adders moving out are $P_B = P_A = P = \text{sump and } x = 0$. Similarly for those moving in, $P_B = P_A = P = P_G$, x = L; the applied pressure P is changed from system pressure to sump in Tseconds. The initial position of the slave piston, x_s , is determined by the positions of the six glob adders. Figure 1 numbers the globs 10, 20, 20', 50, 50', and 100. These numbers determine how many multiples of 0.02 inch each glob moves the slave piston. For example, if at t = 0 the 50 and 20' globs were "out" and the others "in", the slave piston position x_s would be (50 + 20) 0.02 = 1.4 inches. Of course, the velocities are assumed to be zero initially, $\dot{x}_S = y_S = 0$ and $\dot{x} = y = 0$ for all the globs.

Program data

A FORTRAN program for the IBM 7090 was written to solve the system of differential equations describing the actuator model. Considerable experimental data was gathered for this model. The actuator design specifications yielded the values for M, A, L, V_A , V_B , V_C , V_D , M_S , A_{SL} , and A_{SR} . The frictional forces on the glob adders were neglected, but rough measurements were made of the friction of the slave. The fluid used in the actuator was analyzed, and values of the bulk modulus R(P) and density $\rho(P)$ were measured for a few values of P. With these data (1) was integrated to yield f(P) for (2).

Experimentally, the ca for any orifice is calculated from the amount of fluid transferred by a given pressure difference across the opening during some fixed time interval. The pressure differences in the actuator can vary between approximately ± 300 psi, and hence many measurements were necessary in order to reflect accurately the effect of a particular orifice in the model.

One set of data was gathered on each fixed control valve opening for the six glob adders. The needle valve orifice depends on the tuning of the particular actuator. The tuning adjustment is made by turning a screw from its "closed" position any number of turns between 0 and 6. A set of measurements for each of three different settings was compiled on the needle valve mechanism.

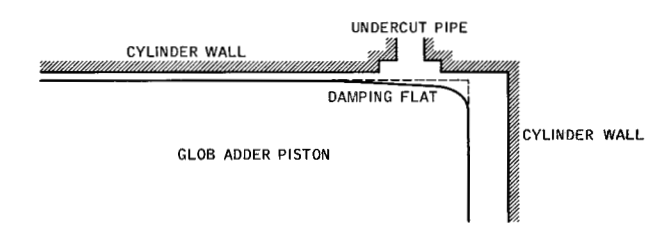


Figure 4 Damping flat.

It is clear from Fig. 4 that the size of the opening through the undercut pipe varies according to the shape of the damping flat and the position of the glob adder piston. The cut of the damping flat on each of the six pistons is different. Measurements of the *ca* were made on the 100 and 50 glob adders with the piston at 16 different positions.

Conclusions

Figures 5 to 8 show the calculated and experimental velocity profiles and the calculated P_D for the 50 glob outstroke, the 50 glob instroke, the 100 glob instroke, and a combination stroke with both the 50 and the 100 globs on instroke.

The actuator model, as one can see from Figs. 5 to 8, displays the major features of the experimental velocity

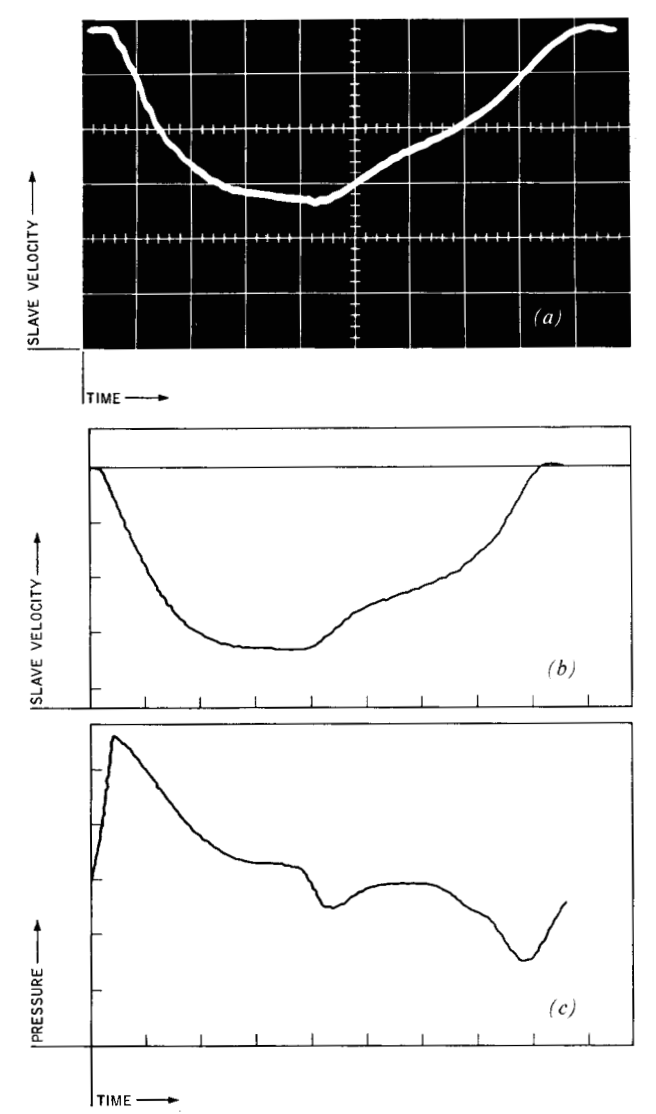


Figure 5 Velocity profiles for 50 glob outstroke.

(a) Experimental velocity trace. (b) Computed velocity curve. (c) Computed pressure in Region D. Scale: Time = 0.01 sec per 0.9 div.; velocity = 5.56 in/sec per 0.9 div.; pressure = 100 lb/in² per 0.9 div.

profiles and it approximates closely the stroke time. Deviations of the computed curves from the typical oscilloscope tracings are most pronounced near the end of the stroke. This can probably be attributed to the fact that the experimental actuator has been carefully tuned to compensate for mechanical tolerances. Various actuators can display quite different velocity profiles before tuning, and experimentally it is known that the actuator is sensitive to the tuning adjustment of needle valves. Limited experimentation with the model indicates that similar compensating adjustments could be made in the model. However, the available experimental data and model

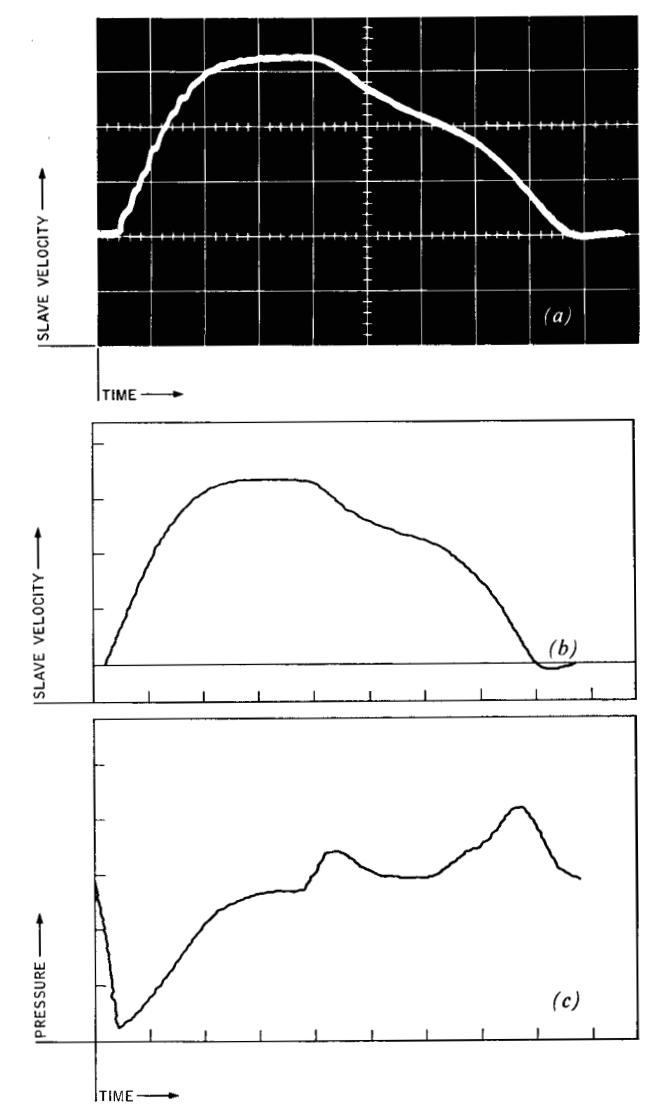


Figure 6 Velocity profiles for 50 glob instroke.
(a), (b) and (c) correspond to the traces in Figure 5, the scale being the same.

assumptions cannot be expected to reproduce the experimental curves to within 5 or 10 percent.

In summary, the model reproduces the experimental curves closely enough to assist engineers in the early stages of design. In particular, stroke times are predicted quite well, and the sensitivity of the end of stroke motion to the shape of the damping flats is shown by the model. The effect of the flow-limiting orifice on the velocity profiles is also reproduced. The time to formulate and program the model was small compared with the effort necessary to determine experimentally the data required for the computation. The basic model and the data collected for it should be of assistance in constructing preliminary models for future hydraulic actuator systems early in the design process in order to pinpoint critical problem areas.

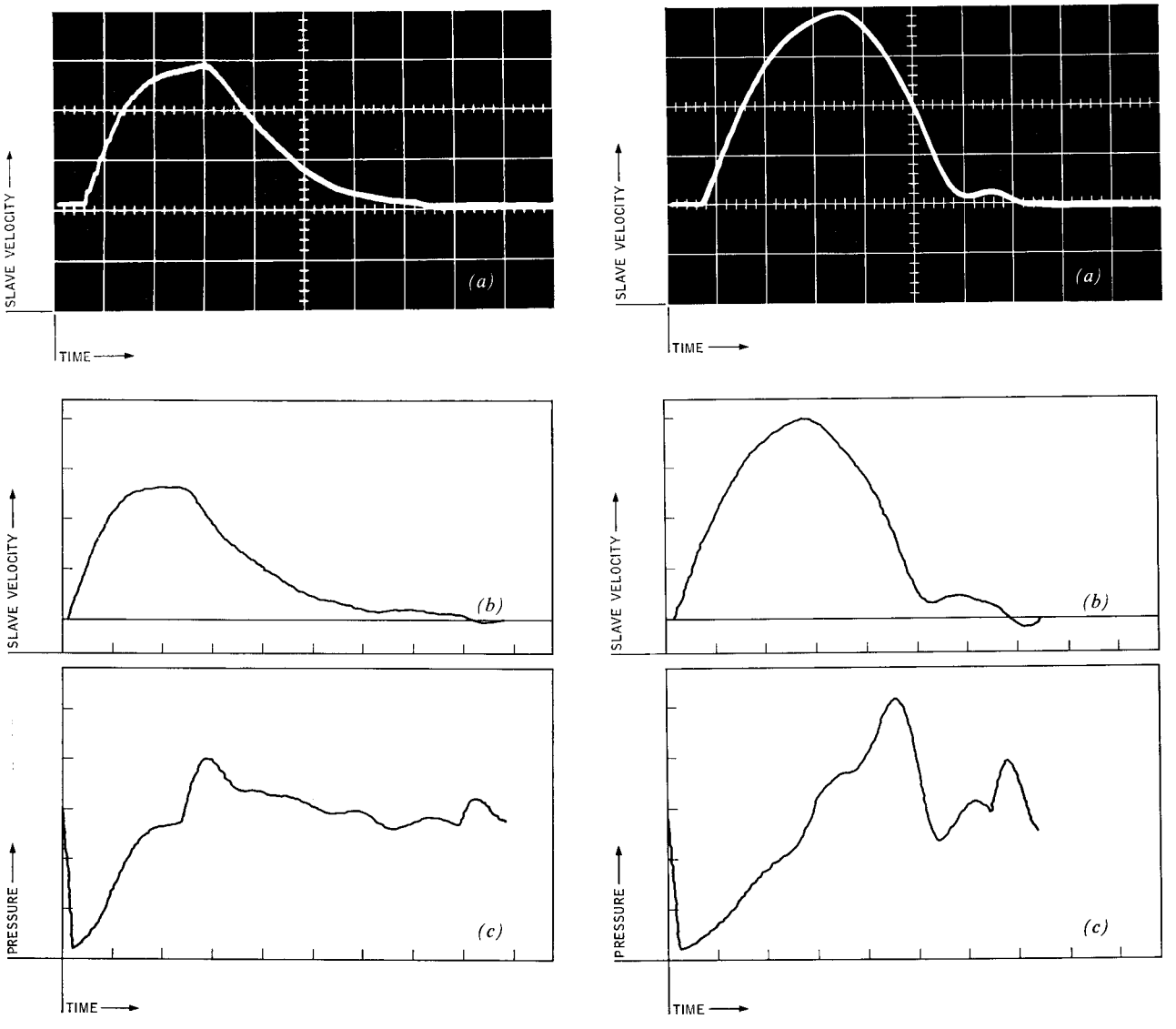


Figure 7 Velocity profiles for 100 glob instroke.

(a), (b) and (c) correspond to the traces in Figure 5. Scale: Time = 0.02 sec per 0.9 div.; velocity = 11.11 in/sec per 0.9 div.; pressure = 100 lb/in² per 0.9 div.

Figure 8 Velocity profiles for 50 instroke and 100 instroke. (a), (b) and (c) correspond to Figure 7, the scale being the same.

Acknowledgments

The authors would like to acknowledge the invaluable assistance of Riyad Abu-Zayyad, James C. Gilmore, and Sam S. Baio, who were responsible for the experimental data, without which the model would not have been feasible. Their numerous suggestions were of great assistance in all phases of the work.

References

1. M. E. Freeman and J. C. Gilmore, "Open Loop Digital Hydraulics Positions Computer Memory Arm," *Hydraulics and Pneumatics* 15, 11 (November, 1962).

- H. T. Albachten and R. C. Treseder, "The Transient Response of Hydraulic Systems, Part I: The Starting Motion," IBM Research Paper RJ-RR-115. December 12, 1957.
- IBM Research Paper RJ-RR-115, December 12, 1957.
 3. H. T. Albachten, "The Transient Response of Hydraulic Systems, Part II: The Stopping Motion," IBM Research Paper RJ-RR-123, May 12, 1958.
- H. T. Albachten, "The Transient Response of Hydraulic Systems, Part III: The Port Sense," IBM Research Paper RJ-138, October 3, 1958.
- J. Regien, "An Investigation of the Stopping Motion of a Hydraulic Actuator," IBM Technical Report TR 02.238, November 9, 1962.
- 6. A. Sommerfeld, *Mechanics of Deformable Bodies*, Academic Press, Inc., New York, 1950, pp. 83-128.

Received November 27, 1963